Available online at www.sciencedirect.com
SCIENCE DIRECT®
International Journal of Mass Spectrometry 244 (2005) 1–14
International Journal of Mass Spectrometry
www.elsevier.com/locate/ijms

SIMION ion optics simulations at atmospheric pressure

Anthony D. Appelhans *, David A. Dahl [1]

Idaho National Laboratory, Chemistry MS 2208, P.O. Box 1625, Idaho Falls, ID 83415, USA

Received 12 January 2005; accepted 30 March 2005

Abstract

A method for simulating the motions of charged particles in atmospheric pressure conditions in electrostatic and magnetic fields has been developed and implemented in a user program for SIMION 7.0 and the predictive capability of the model tested against experiment. The statistical diffusion simulation (SDS) user program avoids the computationally intensive issues of high collision rates by employing collision statistics to simulate the effects of millions of collisions per time step. Ion motions are simulated by a combined viscous ion mobility and random ion jumping approach. Comparison of the model predictions against measurement of Cs^+ transport through room air, N_2, Xe, Ar, and He collision gases in a simple drift cell at pressures from 6 to 640 Torr are favorable and provide confidence that the approach is viable.

Keywords: Ion optics; IMS; SIMION; Ion transport; Ion trajectory simulation

1. Introduction

Motivation: There is no easily accessible, robust, flexible computational tool for predicting the transport of ions in electric and magnetic fields at *atmospheric pressure*, nor which can integrate the pressure-temperature-velocity vector forces of *dynamic gas-flow* with the forces imposed by the electrostatic or magnetic fields to predict the trajectory of ions being transported in such systems. The simple question: "Where do the ions go and why?" cannot be readily answered. This lack of accessible computational and analytical tools restricts our ability to understand the performance of existing instruments, constrains the development of new designs, and hinders the possibility of discovering new phenomena.

Standard mechanistic kinetic collision models [1,2] used in current ion optics modeling programs [3,4] are impractical for use at atmospheric pressure because the number of collisions is so high (∼2 million collisions per mm) that the time to calculate an ion trajectory with a mechanistic collision model becomes unreasonably long (hours per ion). Modeling this process even by Monte Carlo methods can be extremely time consuming, even for the fastest computers. Viscous flow models, while fast, do not account for diffusional effects. The classical approach for modeling ion motion at atmospheric pressure is to use ion mobility (K), which relates the drift velocity (v_d) of the ion to the electric field (E) for a given ion and neutral gas [5]. Thus in a direction where the field is zero the mobility tells nothing about the motion of the ion. However, diffusion theory predicts that the ion will, on average, drift down the concentration gradient, and thus in order to completely model the motion of an ion at atmospheric pressure both the diffusional and mobility terms must be considered. Mobilities have been experimentally determined for many different species in a variety of neutral gases [6,7] and methods for calculating mobility from first principles [8–10] and using statistical approaches [11] have been proposed.

To attempt to predict the motions of ions in a neutral gas at atmospheric pressure, under the influence of electrostatic and magnetic fields, in the presence of other ions (space charge), and with viscous forces accounted for when present, we have chosen to incorporate the mobility and diffusional characteristics in a user program for the SIMION 7.0 ion optics modeling program [12]. This approach enables one to take advantage of the versatility and power of SIMION, including

* Corresponding author. Tel.: +1 208 526 0862; fax: +1 208 526 8541.
E-mail address: anthony.appelhans@inl.gov (A.D. Appelhans).
[1] Retired.

1387-3806/$ – see front matter © 2005 Elsevier B.V. All rights reserved.
doi:10.1016/j.ijms.2005.03.010

the embedded ability to estimate ion–ion electrostatic interactions (space charge), while providing a transparent model for mobility and diffusion that can be readily modified by a user. To enable ion trajectory calculations to proceed at a useful pace (minutes, not days), a statistical approach for calculating the diffusive contribution, based on the ratio of the mass of the ion to the neutral gas and the relative pressure and temperature, has been developed and implemented. In addition, to simplify ease of use, a means to estimate the mobility and the ion radius based on ion mass has been included, with the option of the user defining each of these explicitly if known. These models have been tested against experiment for a number of different neutral gases over a range of pressures with the Cs^+ ion in a simple drift cell. In anticipation of application to fields such as ion mobility spectrometry (IMS) the capability to define either a bulk gas flow, or to define the full three dimensional dynamic flow, along with pressure and temperature, has been included, but not yet tested against experiment.

This paper presents a description of the models and their development, the way in which they are integrated into the ion trajectory calculation, and a comparison of the model with experiment.

2. Overview of mobility and diffusion algorithm development

Statistical diffusion simulation (SDS) is a user program for SIMION 7.0 that simulates motions of charged particles in atmospheric pressure conditions in electrostatic and magnetic fields. It avoids the computationally intensive issues of high collision rates by employing collision statistics to simulate the effects of millions of collisions per time step. Ion motions are simulated by a combined viscous ion mobility and random ion jumping (diffusion) approach. The following sections provide a description of how the algorithms were developed and a diagram showing how these are integrated into an ion trajectory calculation in SIMION. Detailed explanations of the integration into SIMION, particularly the use of arrays of pressure, temperature and flow data, are discussed in the Supplementary material included with this paper or available from the authors on request.

2.1. Ion mobility

The average motion (or drift) of each ion is determined via the user-defined or calculated ion mobility. This is a viscous effect where the force of the electric field is balanced by drag created by the ion's many collisions with the bath gas:

$$\text{Ion mobility velocity}: \quad v_m(\text{cm/s}) = K\frac{d\text{Volts}}{d\text{length}} = KE$$

Where: K = mobility (10^{-4} m^2 Volt^{-1} s^{-1}), E = electric field strength (Volts/m)

The mobility coefficient K is a function of local temperature and pressure. To simplify this effect, the reduced mobility K_o is employed that represents the ion's mobility at standard temperature and pressure (STP): $T = 273.15^\circ$ K and $P = 760$ Torr). The user can define the reduced mobility and diameter for each ion, or the program will estimate these based on the ion mass.

The program looks to see if K_o (reduced mobility) and d (ion diameter) have been defined for each ion mass by the user. The SDS user program assumes that any ion mobility supplied by the user is a reduced mobility K_o (10^{-4} m^2 V^{-1} s^{-1}) appropriate for the collision gas specified. If the user does not define K_o and d, they are estimated during the initialization step. If no K_o was supplied, the value of d will be estimated from the mass of the ion via the formula below. This is taken from the atmospheric aerosols section (14–35) of the Handbook of Chemistry and Physics 83rd edition for negative ions with an average mass = 130 amu, and an equivalent diameter of 0.61 nm used to obtain the mass-to-d scaling constant (it is just an assumption of constant volume density).

$$d_{\text{ion}}(\text{nm}) = 0.120415405\,(\text{mass}_{\text{ion}}(\text{amu}))^{1/3}$$

If the user supplies K_o but not d, the program will use K_o to estimate d. The K_o to d_{ion} formula below was derived by fitting log–log plots of ion diameter and K_o values in air (Handbook of Chemistry and Physics, 83rd ed., pp. 14–36) to a third order polynomial).

$$d_{\text{ion}}(\text{nm}) = 10^{(A)}$$

Where: $A = 3.0367 - 0.8504\ (\log_{10}\ (K_9)) + 0.1137\ (\log_{10}\ (K_9))^2 - 0.0135\ (\log_{10}\ (K_9))^3$ and $K_9(10^{-9}\,\text{m}^2\,\text{V}^{-1}\,\text{s}^{-1}) = 1.0 \times 10^5\, K_o(10^{-4}\,\text{m}^2\,\text{V}^{-1}\,\text{s}^{-1})$.

If the user does not provide K_o, it will be estimated from the d_{ion} value obtained from the above formula. The formula used was derived by fitting log–log plots of ion diameter and K_o values in air (Handbook of Chemistry and Physics, 83rd ed., pp. 14–36) to a third order polynomial:

$$K_o(10^{-4}\,\text{m}^2\,\text{V}^{-1}\,\text{s}^{-1}) = 1.0 \times 10^{-5} \times 10^{(A)}$$

$$\text{Where}: \quad A = 4.9137 - 1.4491\,(\log_{10}(d(\text{nm})) - 0.2772\,(\log_{10}(d(\text{nm}))^2 + 0.0717\,(\log_{10}(d(\text{nm}))^3$$

2.2. Correcting K_o and d_{ion} estimates for buffer gas

The estimating process described above assumes air is the buffer gas (mass = 28.954515 amu and d = 0.366 nm – the SDS default). If the buffer gas is not air then the estimates will be corrected. Note: If both K_o and d_{ion} were defined by the user the SDS program will assume that they are the correct values to use with the buffer gas defined and no corrections will be applied.

$$\text{From gas kinetics}: \quad K_o = \frac{3e}{16N_o}\left(\frac{2\pi}{\mu kT}\right)^{1/2}\frac{1}{\Omega}$$

Where:

$$\mu = \text{reduced\_mass} = \frac{\text{mass}_{\text{ion}} \times \text{mass}_{\text{gas}}}{\text{mass}_{\text{ion}} + \text{mass}_{\text{gas}}}$$

And:

$$\Omega = \text{cross\_section} \approx \pi \left[\frac{d_{\text{ion}} + d_{\text{gas}}}{2} \right]^2$$

Thus K_{ogas} and K_{oair} can be estimated from each other as follows:

$$K_{\text{ogas}} = K_{\text{oair}} C_{\text{gas/air}}$$

$$K_{\text{oair}} = \frac{K_{\text{ogas}}}{C_{\text{gas/air}}}$$

Where:

$$C_{\text{gas/air}} = \left[\frac{\mu_{\text{air}}}{\mu_{\text{gas}}} \right]^{1/2} \left[\frac{\Omega_{\text{air}}}{\Omega_{\text{gas}}} \right]$$

$$C_{\text{gas/air}} = \left[\frac{(\text{mass}_{\text{ion}} \times \text{mass}_{\text{air}}/\text{mass}_{\text{ion}} + \text{mass}_{\text{air}})}{(\text{mass}_{\text{ion}} \times \text{mass}_{\text{gas}}/\text{mass}_{\text{ion}} + \text{mass}_{\text{gas}})} \right]^{1/2} \times \left[\frac{d_{\text{ion}} + d_{\text{air}}}{d_{\text{ion}} + d_{\text{gas}}} \right]^2$$

When d_{ion} is known (or estimated) but K_{ogas} is unknown, K_{oair} is first calculated using the fitting equations described above and then multiplied by $C_{\text{air/gas}}$ to estimate K_{ogas} for the buffer gas.

When K_{ogas} is specified but d_{ion} is unknown a different approach is used. We need an estimate of K_{oair} to use the fitting function to estimate d_{ion}. This requires $C_{\text{gas/air}}$. However, $C_{\text{gas/air}}$ requires knowing d_{ion}. To simplify the calculation an initial estimate of d_{ion} is obtained using the mass of the ion (as described above). This estimate is then used to calculate $C_{\text{gas/air}}$. K_{ogas} is divided by $C_{\text{gas/air}}$ to obtain an estimate of K_{oair}. K_{oair} is then used with the fitting function to obtain the final estimate of d_{ion}.

2.3. Diffusion overview

SDS uses collision statistics to simulate hard sphere collision based diffusion of the ions. Statistically randomized jumps are superimposed on the ion's drift location to combine the drift and diffusion effects. The ion's mass (amu – specified) and diameter (nm – specified or estimated) along with the bath gas's mass (amu – specified) and diameter (nm – specified) as well as the local temperature and pressure are used to estimate the ion's average thermal speed and mean free path (MFP) using basic hard sphere kinetic gas theory. These factors are then used along with the value of the current integration time step to predict the number of expected collisions in the current time step.

A random number is used to obtain a standardized ion jump radius via interpolation between two appropriate statistic tables (selected by the $\text{mass}_{\text{ion}}/\text{mass}_{\text{gas}}$ ratio from five tables for mass ratios from 1 to 10,000, the generation of these tables is discussed later). This standardized jump radius is then scaled by the ion's MFP and the square root of the ratio of the expected number of collisions to the number of collisions represented in each collision statistic table. The result is the radius the ion is jumped. The ion is jumped the specified radius in a random direction from its current drift location. A more detailed description is provided in the Supplementary material.

2.4. Algorithm development

Viscous flow modeling at atmospheric pressures, while fast and simple, lacks the capacity to simulate diffusion effects, which must be included in order to predict the dispersion of a cloud of ions and how the cloud is impacted by electrostatic and magnetic field gradients. It occurred that perhaps a drunkard's diffusion walk approach could be superimposed upon the viscous trajectories by using a statistic of the probability of a radial movement (r_{jump}) as a function the number of expected collisions.

The initial investigation took a greatly simplified approach. The statistic was generated by assuming each ion started at the origin and then moved exactly one unit in a random direction to its next collision point. From that collision point it moved exactly one unit in a random direction to its next collision point. Each ion was flown through a simulated number of collisions (1000) and its final distance from the starting origin (r_{jump}) was recorded. A large number of ions (1,000,000) were flown to obtain a statistic for a probability distribution of r_{jump} given a fixed number of collisions.

The comparison of statistics created for different numbers of collisions (e.g., 10, 100, 1000 and, etc.) uncovered the fact that they followed a square root scaling law. That is, the 50% probability r from the 1000 collision statistic was ~1/10th the 50% probability r from the 100,000 collision statistic. This meant two things. One, a single statistic (using a large number of collisions) could be scaled to represent other statistics with different numbers of expected collisions. Second, the square root scaling would tend to conserve the aggregate r_{jump} accumulated when the expected number of collisions varied (e.g., variable time steps as used in SIMION). This approach looked promising.

To test the consistency a defined mean free path (MFP), ion time step (t), and average thermal velocity (v) were used to estimate the average number of expected collisions in a particular time step. A random number generator [13] was used to pick an r_{jump} value from the probability distribution and then scaled via a square root law:

$$\text{Jump radius}: \quad r_{\text{jump\_mm}} = \text{MFP}_{\text{ion}} \times r_{\text{jump\_distribution}} \sqrt{\frac{n_{\text{expected\_collisions}}}{n_{\text{distribution\_collisions}}}}$$

Where:

$$n_{\text{expected-collisions}} = t_{\text{time-step}} \frac{v_{\text{ion's-average-thermal-speed}}}{\text{MFP}_{\text{ion}}}$$

A random direction was chosen and the ion was jumped (instantaneously) a distance of r_{jump}(mm) to its new position. This process was repeated at each time step throughout the ion's trajectory. Experiments with smaller and larger time steps verified that the diffusion rate of ion trajectories appeared to remain independent of the chosen time step. The model predictions were compared to the results obtained from the more classical Monte Carlo collision model [1]. Initial results indicated that the r_{jump} statistical approach was very promising.

2.5. Mass ratio and development of scaling laws

All of these approaches assumed that the ion and gas molecules were identical (e.g., the mass ratio = 1). To explore the effects of mass ratio a series of r_{jump} statistic generating programs were created to model hard sphere impacts in a Monte Carlo manner. The general observations were consistent with one's intuition from basic physics: When the mass ratio is one, a single collision can randomly kick an ion off with a new kinetic energy and random direction of travel. However, if the ion is 10,000 times the mass of the neutral gas molecules it takes thousands of collisions to totally randomize (de-correlate) its initial velocity. Thus a heavy ion tends to retain its initial velocity largely unchanged through many collisions (linear r scaling region). However, as the number of collisions mounts the velocity de-correlates to the point that r begins to scale as the square root as described above (desirable).

Two collections of simulations were run in order to obtain a better understanding of the process. The first collection of simulations, referred to as fixed, always initialized each ion with a fixed velocity of 1 along the x-axis, and always used a fixed time step between collisions of 1. The second collection of simulations started each ion out with a random Maxwell Boltzman velocity (average distribution velocity normalized to 1) in a random direction, and each time step between collisions was Poisson randomized to an average of 1 (normalized). The ions collided with gas molecules having random flight directions and randomized Maxwell Boltzman energies of the same average temperature of the ions (v_{avg} gas/v_{avg} ion = sqrt (mass ion/mass gas)). A separate simulation was run for each of five different total numbers of collisions (10, 100, 1000, 10,000, or 100,000), and had one of seven mass ratios (1, 10, 100, 1000, 10,000, 100,000, or 1000,000). Thus each collection had 35 simulations.

The plot in Fig. 1 compares the variation of the 50% r distribution point for the fixed and random collections of simulations. The most important observation is that both collections with the equivalent mass ratios converge to common r (50%) values when the number of collisions is large enough. This means that both approaches lead to the same r statistics for large values-of-n collisions. Also notice that the lower mass ratios converge at a lower number of n collisions.

The results shown in Fig. 1 indicate that if the number of collisions is high enough, ~100,000, mass ratios of less than 10,000 to 1 will have converged into the square root law. This means that if the time steps in a trajectory calculation are large enough for 100,000 collisions to occur we can ignore the linear rule region and assume the ion trajectories will be fully de-correlated and fly in the square root law scaling region. This condition is easily satisfied for ions flying in atmospheric conditions using the sub to one mm integration steps typically used.

The question remained as how to scale between mass ratios. Initial evidence indicated that two ion simulations of 100,000 collisions per ion and mass ratios 1 and 10,000 might scale linearly on a log–log plot. A more detailed check showed (Fig. 2) that mass ratios of 10 and 100 deviate by 20% or so from the simple linear assumption. In order to reduce these errors, five 100,000 ion by 100,000 collisions per ion simulations (at 1, 10, 100, 1000 and 10000 mass ratios) were run to create a master set of scalable statistics. These are then applied to calculate jump radius (due to diffusion) at each time step.

The jump radius for a given mass ratio is determined by linear interpolation. The interpolation scheme involves using a random number to select the distribution percentage, getting

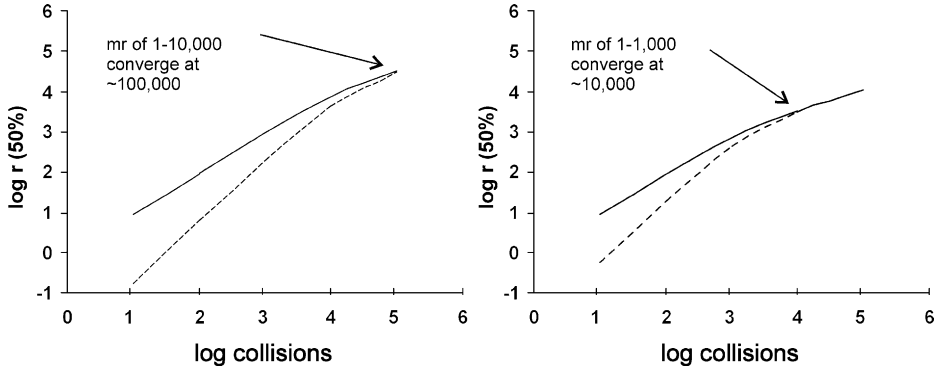

Fig. 1. The 50% radius value of the diffusion distributions for a fixed velocity and distance step (dashed line) and a Poisson randomized step (solid lines), illustrating that the two converge to a common value when the number of collisions is high enough relative to the mass ratio of the two colliding particles.

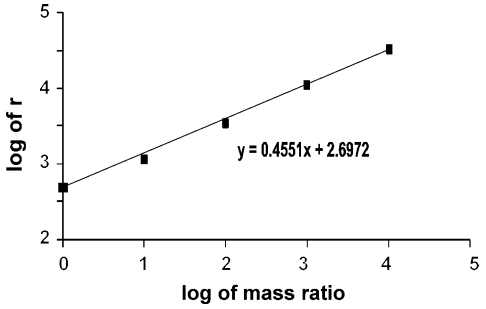

Fig. 2. Jump radius as a function of the mass ratio. A piecewise linear interpolation is used to determine the jump distance for mass ratios between each decade of mass ratios.

the $\log_{10}$ of the collision mass ratio (mr), using it to select the two adjacent distributions, extracting the r value from each distribution, taking the $\log_{10}$ of each r value and using linear (log–log) interpolation to get the r. The result is raised to the 10th power to get r_{obtained}.

$$\log(r_{\text{jump\_obtained}}) = \log(r_{1\text{jump}}) + 0.39(\log(r_{2\text{jump}}) - \log(r_{1\text{jump}}))r_{\text{jump\_obtained}} = 10\log(r_{\text{jump\_obtained}})$$

This $r_{\text{jump\_obtained}}$ value is then square root scaled to the expected number of collisions:

$$\text{Jump radius}: \quad r_{\text{jump\_expected}} = \text{MFP}_{\text{ion}} \times r_{\text{jump\_obtained}} \sqrt{\frac{n_{\text{expected\_collisions}}}{n_{\text{distribution\_collisions}}}}$$

Where:

$$n_{\text{expected\_collisions}} = t_{\text{time\_step}} \frac{v_{\text{ion's\_average\_thermal\_speed}}}{\text{MFP}_{\text{ion}}}$$

MFP_{ion} = mean free path of the ion

We then have the distance the ion will be moved due to diffusion; the direction is determined using a random number. The ion's viscous velocity, determined previously with respect to the electric and magnetic forces and any applied gas velocity vectors, is not modified in this step.

2.6. Interaction of SDS user program with SIMION

The implementation of the user program in SIMION is best described using a flow diagram. Fig. 3 shows a flow diagram of the trajectory calculation segment of SIMION and where at each step the information from the SDS user program is included.

3. Space charge issues

The large numbers of collisions that occur at atmospheric pressure result in typically very low ion velocities (relative to vacuum conditions), even in strong electric field gradients. One consequence of this is that space charge interactions become more significant, and can easily become the dominant force. Thus practical use of the SDS method requires the ability to at least estimate the effect of space charge on the ion trajectories. SIMION 7.0 includes two methods for estimating space charge effects; ion beam repulsion and ion-cloud repulsion. The ion cloud repulsion methods (coulombic and factor repulsion) will work with SDS because they are based on a time-coherent approach, but the beam repulsion method does not support random jump effects since it is based on a space coherent assumption. These methods are discussed in detail in the SIMION users manual [12]. These methods have proven useful under vacuum conditions in estimating the onset of space charge effects, and, in limited cases where the space charge is not too severe, seem to predict relatively well the observed behavior, but they have one distinct limitation. That is, only ion–ion interactions are accounted for; the effect of the charge density on the local electric field is not computed. The electric field forces on an ion from all of the other ions and the forces arising from the fields of the electrodes are simply superpositioned. This ignores the shielding effect on an ion in a high charge density region. So for example, in an area where the charge density is high (at the face of a thermal emitter), the field used in SIMION to calculate the trajectories does not include the perturbation of the field due to the charge density, nor is the shielding effect of the charge density on the ion taken into account, and thus the ion trajectories calculated in this type of region should be viewed with skepticism. In vacuum conditions the ion velocity can increase quickly as the ions leave the emitter, and thus the time for interactions is reduced. However, at atmospheric pressures the high collision rate keeps the ion cloud velocity low, and thus the time for interactions increases. Thus while a beam diameter may increase a few percent in a few centimeters under vacuum conditions, at atmospheric conditions it can increase by orders of magnitude in this same distance. Thus one must carefully examine this aspect when applying the SIMION space charge models with the SDS method. Ignoring the space charge effect altogether is not a viable solution. Incorporating it fully using a Poison calculation is beyond the scope of SIMION. Our experience in using the SIMION coulombic space charge model with the SDS model and comparing it with experimental results has convinced us that if one takes care to understand where these effects might be occurring there are strategies that can accommodate the effect and allow useful simulations. Further discussion is included in the Section 6 of this paper.

4. Experimental

To provide well characterized data against which the SDS model could be tested an instrument was constructed to measure the spatial distribution of ions emitted from a thermal source and subjected to an electric field gradient in a diffu-

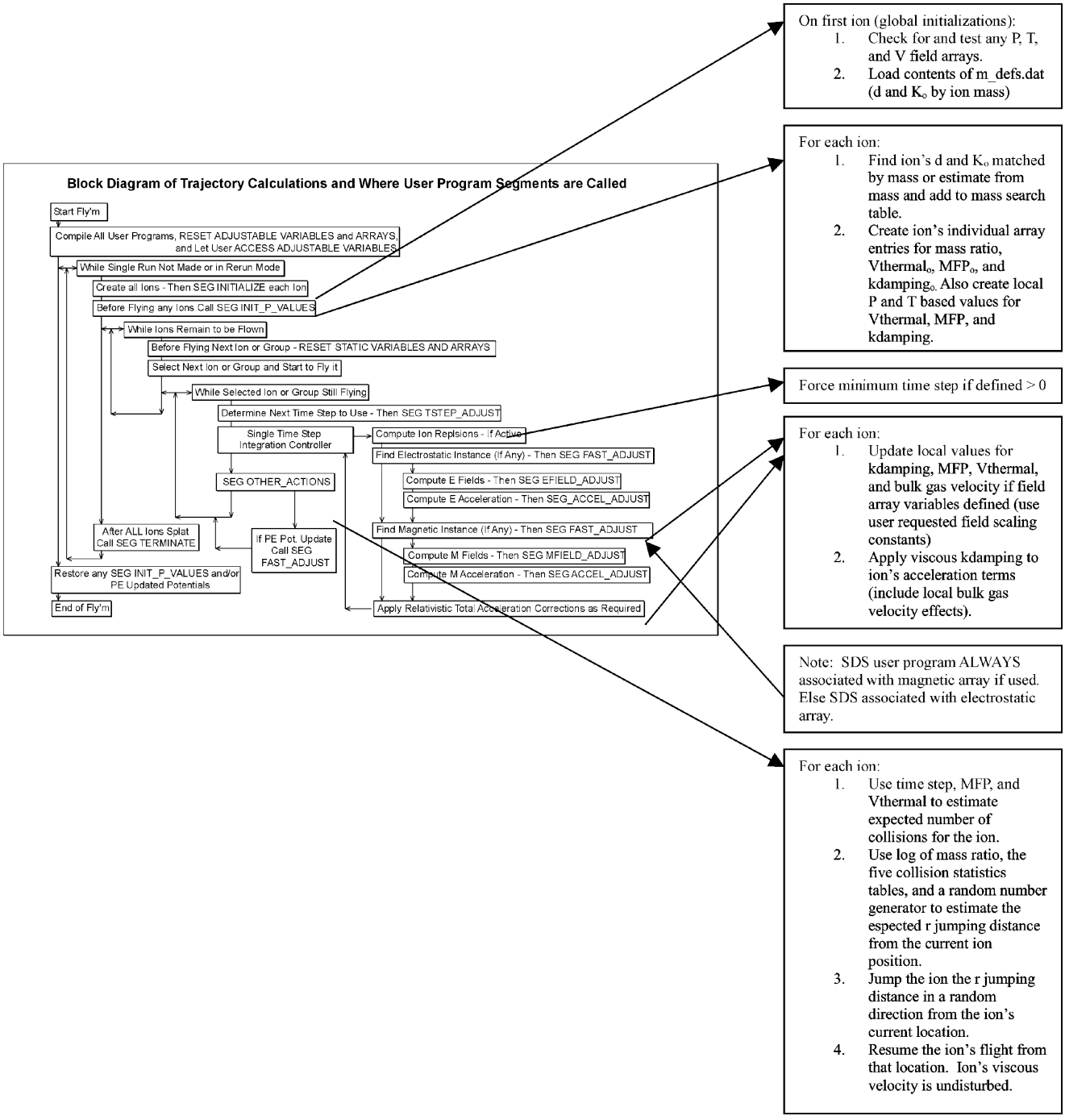

Fig. 3. Block diagram of the trajectory calculation routine in SIMION and the points at which the SDS user program interacts with the main program.

sion/mobility drift cell which could be filled with different gasses at pressures ranging from 6 to 640 Torr (atmospheric pressure in Idaho Falls). The vacuum system was pumped with a turbo pump and had a gas manifold for varying composition and pressure of the gas in the system. When filling the system with a gas the system was first pumped to a vacuum of $\sim 10^{-5}$ Torr or better, the chamber was isolated with a gate valve, and gas of the desired composition was introduced via a leak valve. The absolute pressure in the chamber was measured with a calibrated capacitance manometer (MKS PR 4000). Room air, dry nitrogen, helium, argon and xenon collision gases were used. The pressure range of 6–640 Torr and the field gradient (from 10 to 250 V/cm) kept the experiments within the low-field mobility region [5] for which the model assumptions are appropriate.

The drift cell, shown in Fig. 4, consisted of a thermal ion source mounted behind a plate containing a small aperture (3 mm) through which the ions entered the drift region. Up to

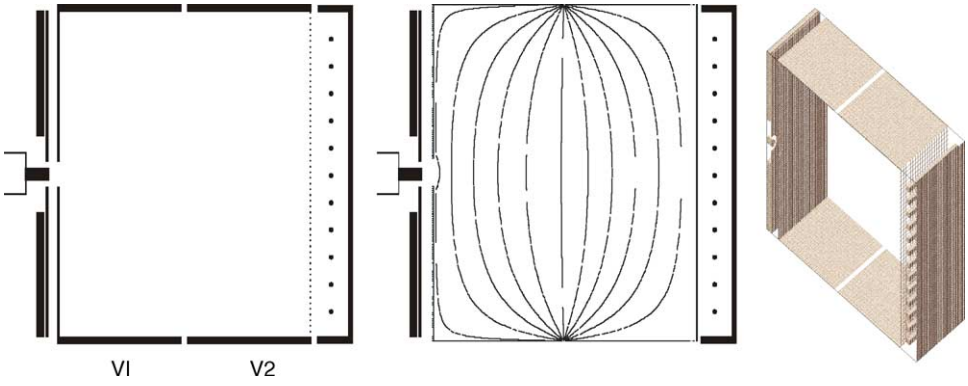

Fig. 4. Cross section of the drift cell (left) and the equipotential contour in the cell (middle) and an isometric view of the middle region of the cell.

4 rectangular sections, square in cross section (50 cm) could be connected to the ion source plate and collector plate to provide different length drift regions. The voltage gradient across the cell was generated by holding one half of the cell at one potential (V_1) and the other half of the cell at a second (lower) potential (V_2). This produced a relatively flat and linear gradient through the center of the cell. The ion spatial distribution was measured at the end of the drift region using a series of parallel wires individually connected to electrometers. The wires were behind a guard screen (95% pass rectangular grid) that defined the electrostatic end of the field gradient in the drift cell. A second guard plate was located behind the wire array. By operating the guard screen and guard plate at a potential above the wire array (ground) the ions that passed through the guard screen were attracted to the wires and measured to determine the distribution of the ions in the ion cloud.

There were two modes for measuring the current on the wires. In mode 1 a single electrometer was used to serially measure the current on each wire while the remainder of the wires were grounded (so as not to perturb the ion distribution). Mode 1 could only be used for conditions of atmospheric pressure in air as the vacuum system had to be open to allow the electrometer lead to be moved from wire to wire. In mode 2 five separate electrometers were connected to the wire array and the current on the wires was measured simultaneously. This mode allowed the pressure to be reduced below atmospheric and the use of gases other than air. Measurements were made to verify that the two methods were equivalent.

The ion source consisted of a stainless steel tube packed with a Cs–zeolite material. The tube was spot welded to a chromel heater wire. The ion source was tested in a mass spectrometer to verify that the emission was >95% Cs^+ (under vacuum conditions) prior to use in the drift cell. We have not experimentally confirmed this emission composition at atmospheric pressures, but our results are consistent with the assumption that the major fraction of the ions are Cs^+. The temperature of the ion source at which measurable currents were produced varied with the composition of the gas in the cell and the pressure (due to the different thermal conductivity of the various gases used).

The geometry of the source region was configured to minimize the effect that the voltage of the emission source had on the gradient in the drift cell. The voltage of the emission tube changed as the gas composition and pressure changed because the current through the heater wire had to be varied significantly to maintain the desired emitted ion current. The geometry illustrated in Fig. 4 minimizes the effect of this change on the drift cell field gradient, although there was some evidence with Xe that space charge in this region could effect the ion distribution (discussed later). The same ion source was used in all of the experiments. A method for estimating the emitted current was developed and is described further in the Section 6.

Experiments were conducted by evacuating the chamber and then filling the chamber with the desired gas to the desired pressure, heating the filament and monitoring the output to assure it was stable, setting the voltages on the drift cell to obtain the desired field gradient, and then measuring the current on the wire array. In mode 1 the current was measured in the sequence of wire 1 to wire 11 then back and the two signals averaged. In mode 2 the electrometer readings were recorded simultaneously (by hand). Tests were conducted to determine that the electrometers gave equivalent readings independent of which wire they were connected to (which implies they all have nearly the same input impedance).

5. Simulations

The SIMION 7.0 program [3] was used for all simulations. The drift cell was modeled in full three-dimensional geometry. The values used for the reduced mobility and atomic diameters for Cs^+ in He, Ar, Xe, N_2 and air are shown in Table 1 along with the reference.

Ions were generated at random positions on the ion source emission surface and flown in 6 groups of 50 ions each that were emitted over a fixed time window of 1 ms, each group separated by 0.2 ms. The staggered groups produced

Table 1
Reduced mobility (K_o) and collision diameter (nm) for Cs^+ in the test gases; references are in brackets

	He	Ar	Xe	N_2	Air
K_o (Cs^+)	18 [14]	2.1 [15]	0.9 [15]	3.3 [16]	1.36 [17]
d (nm)	1.9 [17]	2.8 [17] 3.16 [16]	3.4 [17] 4.2 [16]	3.15 [17] 3.6 [16]	3.15 [17]

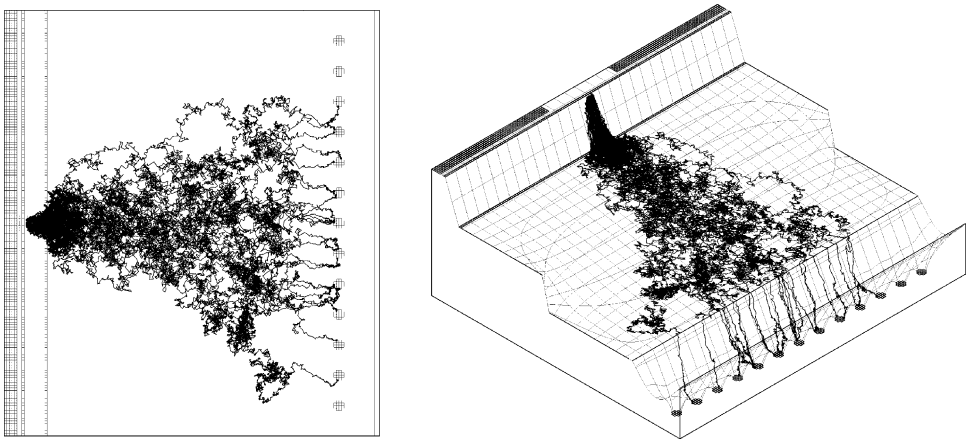

Fig. 5. Calculated ion trajectories for Cs^+ in the drift cell at atmospheric pressure illustrating the dispersion of the ion cloud and the collection of the ions on the wire array (left). Potential energy plot with equipotential contours (right).

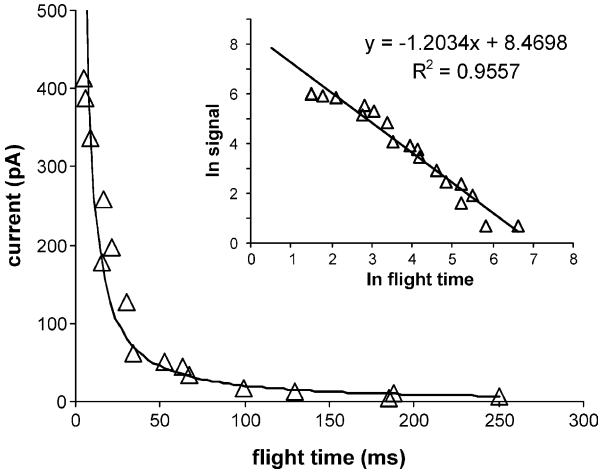

Fig. 6. Measured total current at the wire array as a function of the ion flight time for room air at atmospheric pressure.

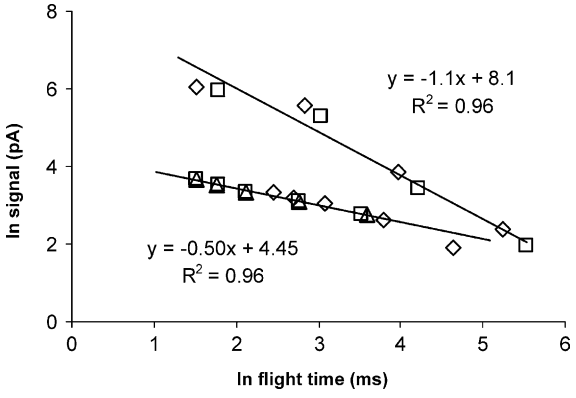

Fig. 7. Measured total current at the wire array as a function of the ion flight time for filament currents of 2.3 (lower) and 2.6 (upper) amps and best fit lines for each.

a “beam” of ions of a given time length, which enabled the axial effects of ion–ion interactions to be more realistically modeled. The coulombic repulsion space charge option was used and the total current was adjusted to that measured in the experiment. In this option the total charge is divided among the ions at time = 0 and the trajectory of each ion (cloud) takes into account the forces due to all of the other ions (clouds of ions). As noted previously the effect that the charge would have on the local electric field is not taken into account. Fig. 5 shows a cross section of the SIMION model of the drift cell and a representative set of ion trajectories on the potential energy surface.

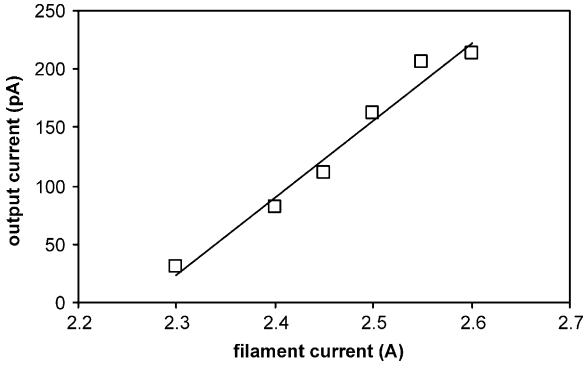

Fig. 8. Total measured current at the wire array as a function of the filament current.

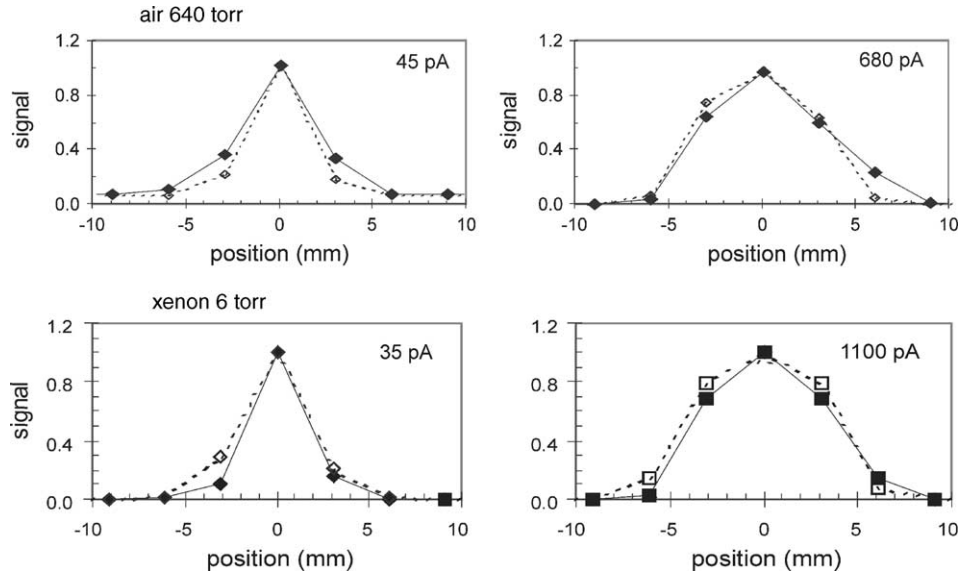

Fig. 9. Measured (solid) and predicted (open dashed) beam profiles at different beam currents for Cs^+ in air and xenon at a 120 V/cm gradient. (Normalized to maximum).

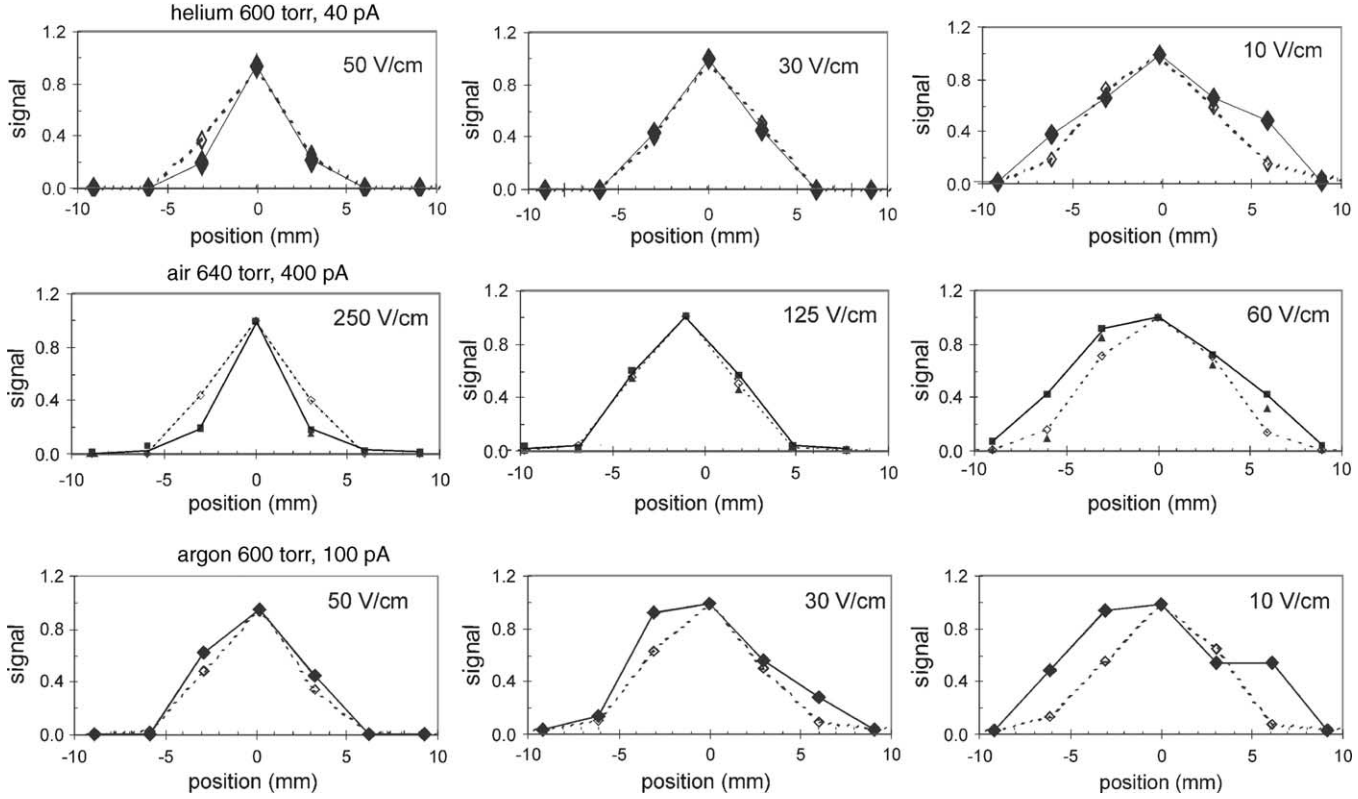

Fig. 10. Measured (solid) and predicted (open/dashed) beam profiles for Cs^+ as a function of the voltage gradient (flight time) for three collision gases. (Normalized to maximum).

6. Results

6.1. Beam current initial conditions and lifetime analysis

It was observed that the total ion current measured on the wire array was dependent on the drift time. Since the ion beam was not diverging to the point where ions would hit the walls rather than the wire array, the conclusion was that some neutralization or charge exchange mechanism was occurring. To accurately model the experiments a good estimate of the beam current at the source aperture location was required. Thus to estimate the starting current based on the current measured at the wire array the ion losses had to be accounted for. To do this the beam current was measured as a function of the flight time from the ion source to the wire array and this data was fit to an equation that was then used to extrapolate back to the start time.

The beam current was measured at several different filament currents, corresponding to different ion current output levels, and the flight time was varied two ways: by changing the voltage gradient between the aperture plate and the wire array where the beam current was measured, and by changing the physical length of the drift cell (from 12.5 to 50 mm in 12.5 mm increments). The SIMION model was used to calculate the flight time given the voltage gradient and drift cell length (since the gradient was not perfectly linear, particularly near the aperture, a SIMION calculation was deemed more accurate than a simple scaling by gradient). Fig. 6 shows the results of these measurements for four different drift cell lengths at 5 different voltage settings. Data taken at several other filament currents showed the same trend. Fig. 7 presents the measured beam current as a function of lifetime plotted as the natural log of each, for two different filament settings, 2.3 and 2.6 A. Also shown are the best-fit equations for each

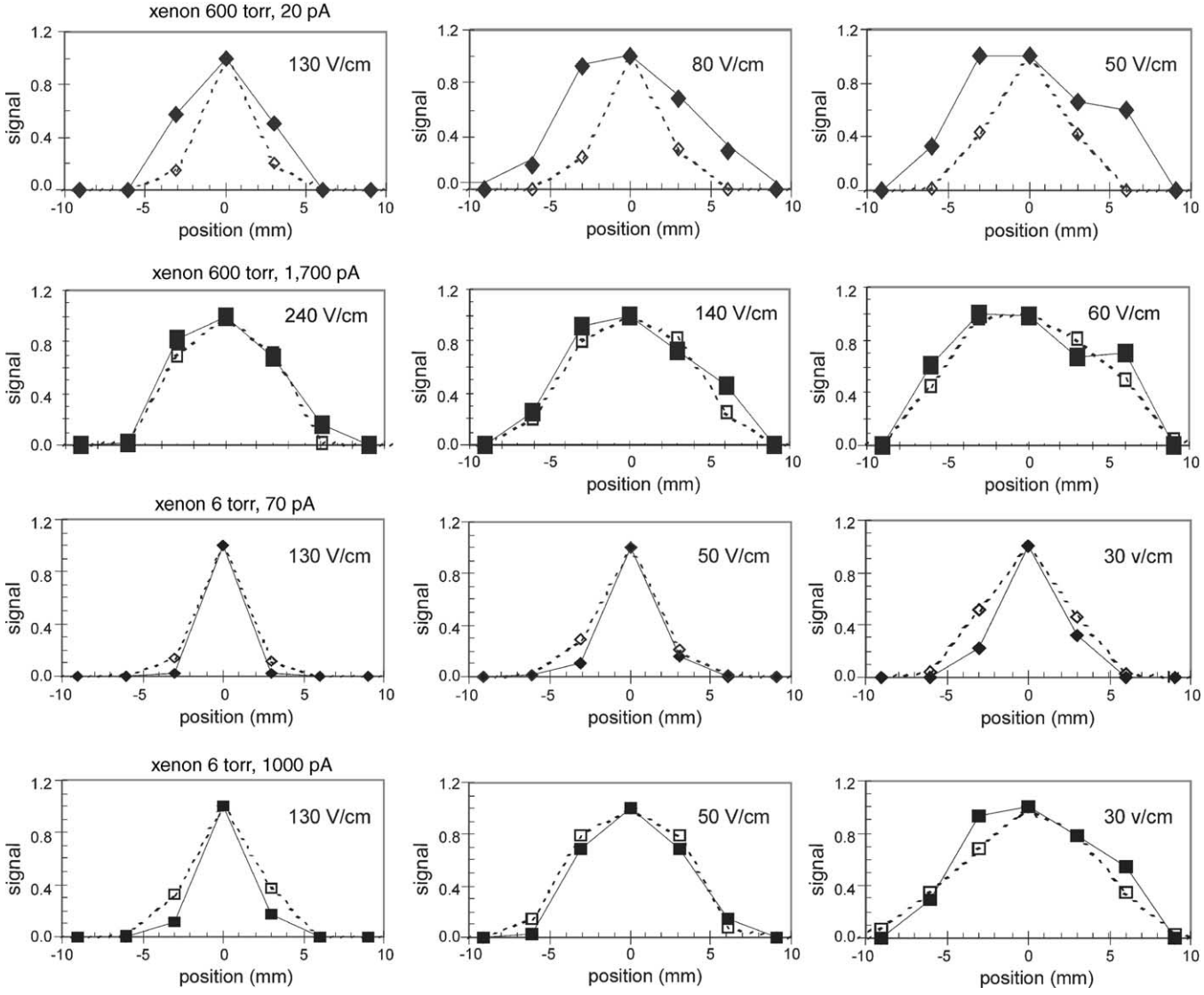

Fig. 11. Measured (solid) and simulated (open/dashed) beam profiles at various field gradients in the 25 cm cell with xenon collision gas. (Normalized to maximum).

data set. By extrapolating to time zero the total ion output from the source can be estimated. The fact that the slope of the two lines is not the same indicates that the stability of the ions is probably a function of their initial temperature (not surprising). The fact that there are no discontinuities in slope indicates that there is probably only one major loss mechanism. There are a variety of potential loss mechanisms, ranging from ion molecule reactions to simple ion molecule charge exchange, any of which can lead to neutralization of the Cs^+ ions.

The output ion current for other filament currents was estimated assuming the output was linear with filament current. To assess this a series of beam profile measurements were made in which the voltage gradients were kept constant and the filament current was varied. The total beam current was determined by integrating the beam profile for each filament current setting. Fig. 8 shows the result for the 25 mm drift cell and a 130 V drop from the aperture plate to the wire array guard grid.

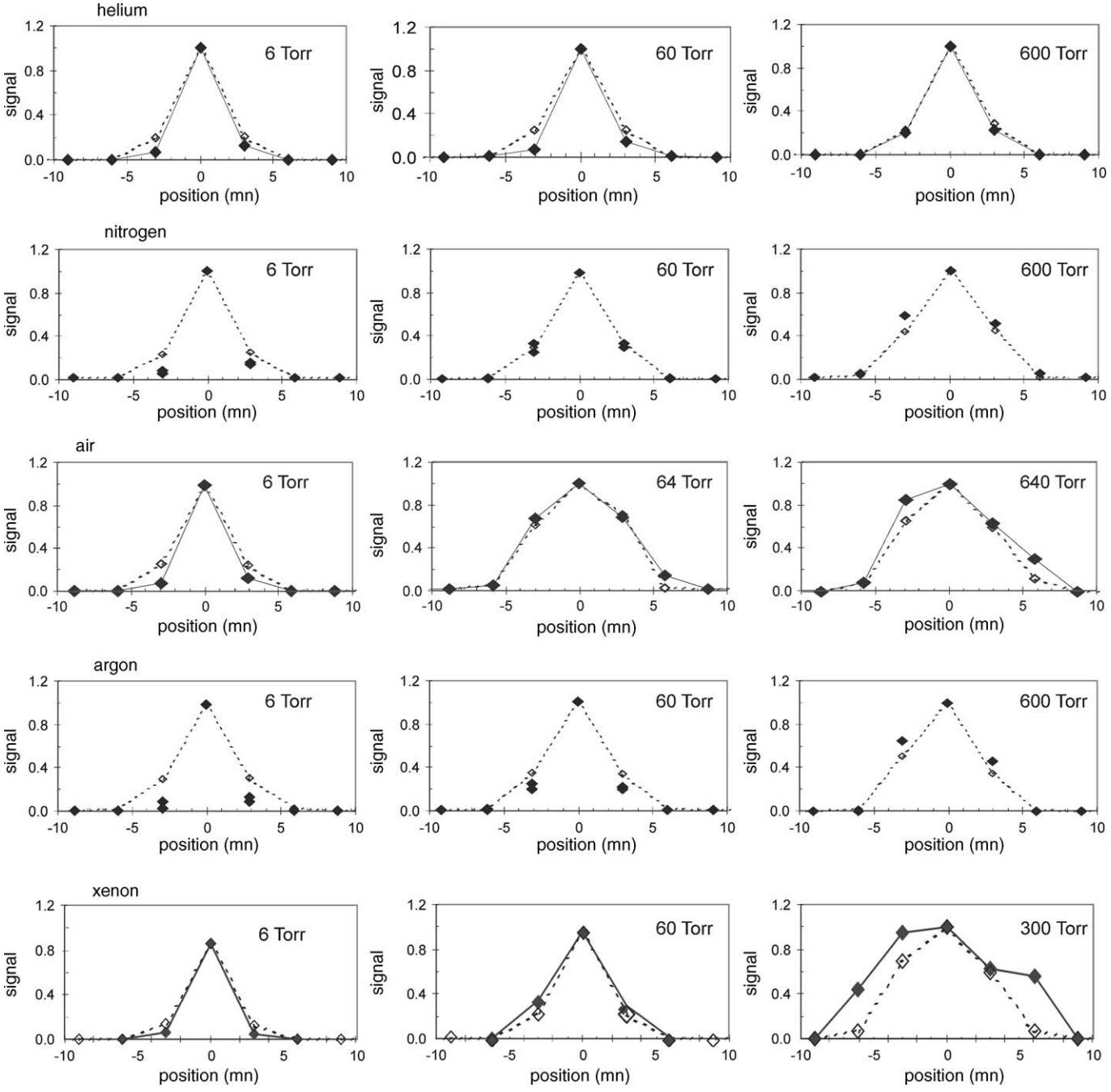

Fig. 12. Measured (solid) and predicted (open/dashed) Cs^+ beam profiles in different collision gases over a range of pressures. (Normalized to maximum).

6.2. Space charge effects

Initial measurements clearly showed that the beam dispersion was dependent upon the ion current, dispersion increasing as the ion current increased indicating that space charge forces were influencing the dispersion. Using the 25 mm length drift cell the beam current profiles were measured for a series of beam currents with each of the collision gases. The coulombic space charge model in SIMION was used in conjunction with the SDS model to predict the beam current profiles at the various ion currents. The amplitude of the current at the source aperture used in the model was based on the method described previously, correlating beam current at the aperture with filament current. Representative examples in air and in xenon at a gradient of 120 V/cm. are shown in Fig. 9. The agreement between the model and experiment was good for all of the cases studied over a fairly large range of beam currents. Additional examples and discussion are included in the next section.

6.3. Varied voltage gradient (drift time)

Measurements of the beam dispersion as a function of the drift time (voltage gradient) at a constant beam current for helium, air and argon in the 25 mm drift cell are shown in Fig. 10. As expected, as the drift time is increased the dispersion of the beam increases. The measurements with air were made two different ways; in one a single electrometer was used to measure the current on a single pin, while all of the other pins were grounded (filled squares), in the second method (filled triangles) a separate electrometer was connected to each of pins 5 through 9 and the current on each pin was measured simultaneously. The results show that the two measurement methods are consistent. The measurements with the argon and helium were all made with the multi-electrometer method. The simulations were performed with initial beam conditions (current and diameter at the aperture) based on the method described previously. The agreement is reasonably good, the largest deviations between the measured and simulated dispersion occurs for the longest drift times (lowest gradients).

The results for xenon collision gas showed an anomaly for very low beam currents at a high (600 Torr) pressure, as shown in the top set of graphs in Fig. 11 (600 Torr, 20 pA). Both the measured and predicted dispersion increase with decreasing field gradient (increased flight time) as would be expected, but the degree of the dispersion is consistently under predicted. This was not observed at higher beam currents or at lower pressures, as shown in the bottom three sets of graphs in Fig. 11. Further simulation analysis showed that increasing the voltage on the filament and plate to simulate the possible effect that space charge might have on the field in the region between the ion source and the aperture caused the beam to broaden out (similar to the effect seen in the experiments). If the space charge in this region distorts the field and makes the field at the aperture more of a hill, then the ions would spread out more as they leave, leading to the increased spread as seen in the top line of graphs in Fig. 12. It appears likely this is what is happening and is probably an example of where the space charge method used in SIMION is not sufficient, because the effect the charge density would have on the field is not taken into account in calculating the trajectories. Thus even though the ion feels the force of the other ions, the field at that position was calculated assuming zero charge density. At higher ion currents the measured results at three different filament temperatures and at three different sets of voltages in the filament region showed that the beam dispersion was independent of the current, that is, the space charge at the aperture dominated the beam spread and the field between the source and the aperture was not very important. This would be exacerbated with Xe, and minimized with He, consistent with our measured results. Unfortunately we see no way to quantify this with the existing system; it would require redesign of the source region to shield the diffusion field (post aperture) from the space charge field near the source. This behavior was not observed with the other collision gases and except for this one case the agreement between the measured and predicted dispersion over the range of collision gasses and pressures tested was quite good.

6.4. Varied collision gas pressure and composition

The effect of the fill gas pressure and composition on beam dispersion was measured for pressures ranging from 6 Torr to atmospheric with helium, air, nitrogen, argon and xenon collision gas. Because the output of the ion source is dependent upon the pressure and the fill gas composition, the filament current was adjusted so that the measured ion current on pin 7 (the center pin) was approximately the same for each pressure. The current used for the simulation was

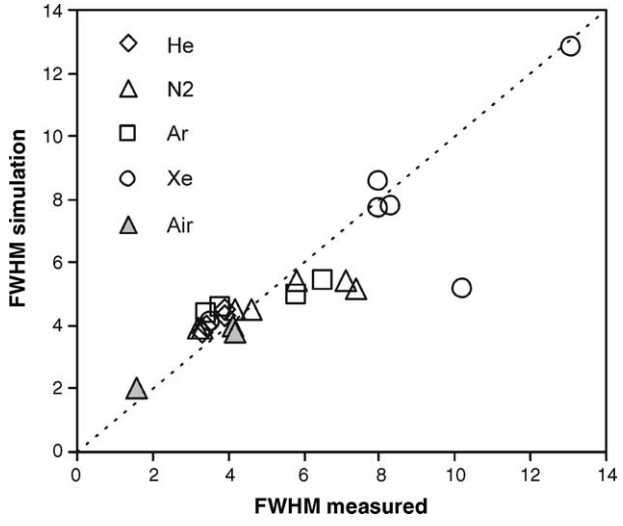

Fig. 13. Predicted versus measured FWHM of the Cs^+ beam profile for the five different collision gases at pressures ranging from 6 to 640 Torr.

determined using the method described previously. Fig. 12 shows the measured beam profiles and the simulation results. The K_o and d values used in the simulation were taken from Table 1.

A summary of the ability of the SDS model to predict the beam dispersion over the pressure range of 6–600 Torr for the four collision gases tested is presented in Fig. 13 in which the predicted FWHM is plotted against the measured FWHM. Except for the 600 Torr Xe data outlier at low current (20 pA), the model predicts the data reasonably well.

7. Discussion and conclusions

The SDS model combined with the coulombic space charge model in SIMION appears to predict the combined effects of mobility and diffusion on the trajectories of an atomic ion at pressures ranging from 6 Torr to atmospheric (640 Torr) in a simple drift cell. The fact that the model predicted the dispersion of the beam over this wide range of pressures and for collision gasses ranging from 4 to 131 amu is very encouraging. It was clear that at atmospheric pressure levels the effects of space charge were significant and must be taken into account. The beam currents at which space charge became significant were lower than our previous experience at high vacuum conditions would have suggested. In our experience, for small diameter beams (∼1 mm) in the keV energy range in vacuum, space charge effects were not significant until the beam current was ∼100 nA. Whereas at atmospheric conditions the onset occurred at least several orders of magnitude lower. Thus application of the model must be critically evaluated with this in mind.

The published mobility of Cs^+ in the gases tested ranged from 0.9 to 18, a factor of 20; this seems a good test of the model, and points out that these parameters are critical for producing accurate simulations. Within the field of ion mobility spectrometry the mobility of a wide range of molecules have been experimentally determined and are available in the literature; thus the basic data needed for applying the model seems accessible.

As with most ion optics trajectory simulations the outcome is very sensitive to the initial conditions (ion starting position, charge density) and the results can be significantly altered by relatively small changes in the initial conditions. This is not a shortcoming of the method, but reflects the actual sensitivity of the ions to these conditions. Thus users are cautioned to carefully and critically evaluate the accuracy of their knowledge of the initial conditions in assessing the usefulness of the predicted ion behavior.

7.1. Magnetic fields

SDS is capable of including magnetic fields in the simulations providing a few limitations are recognized. Once the ion is at thermal equilibrium with the other molecules in the gas (which happens quickly at atmospheric pressure) its average velocity will be the average thermal velocity and essentially constant. The velocity at any particular time step could vary from the average within the Boltzman distribution, but its velocity during a single time step is constant, and thus any force due to its velocity is constant during the time step. An ion moving at a constant velocity in a uniform magnetic field experiences a force that imposes a circular trajectory (orbit) if there are no other electrostatic forces acting on it. The magnetic orbit will have a radius equal to the thermal cyclotron radius for the ion at that temperature and B field. If the mean free path between collisions is very short relative to the ion's thermal cyclotron radius, the arcs of the ion's trajectory circles become virtually straight lines. In this case there is almost no difference between the non-magnetic and magnetic trajectories. For example, a nitrogen molecular ion in nitrogen gas at 25 °C and atmospheric pressure has a mean free path (mfp) of approximately 6.76×10^{-8} m. If it is in a 7 Tesla field its thermal cyclotron radius (rcyc) is 1.979×10^{-5} m. The ratio mfp/rcyc is then 3.41×10^{-3}, a very small arc – basically a straight line. Thus the ion diffuses almost identically to a non-magnetic situation. SDS can probably predict the viscous *and* diffusion effects reasonably accurately in this situation. However if the pressure was 0.001 atmospheres the ion would make slightly more than half of a thermal cyclotron orbit between collisions, and the arc no longer approximates a straight line. In this case SDS might estimate the viscous trajectory reasonably well, but it would tend to overestimate the diffusion. These issues must be kept in mind when conducting simulations with SDS and magnetic fields. A series of examples illustrating these issues are available from the authors.

7.2. Bulk gas flow and local temperature and pressure options

As alluded to in the introduction, the SDS user program allows a bulk gas flow to be defined and then applied in the trajectory calculation. The local 3D rectangular coordinate values of the bulk gas velocity are subtracted from the damping velocity before the acceleration due to damping is calculated. This provides a simple method for simulating the effects of a bulk gas flow, for example what one might encounter in an ion mobility spectrometer in the drift tube (counter-current flow). This has not been tested against experiment but has been tested against simple, well-understood bulk flow conditions and produces the expected behavior. In addition to bulk gas flow there is the capability for the user to define pressure, temperature and bulk gas velocity fields via five specifically named arrays. Thus if the pressure, temperature and flow as a function of position have been determined for a specific geometry (by some other modeling program), they can be integrated into the trajectory calculations. Details of this are provided in the Supplementary material to this paper. One caution; in SIMION all conditions are assumed constant

over a time step, thus if the gradient of the pressure or temperature were high relative to the distance an ion traveled in a time step, such that there was a significant change over the distance an ion traveled, the current SDS model would not account for the effects of the gradient. To account for the effects of strong gradients the SDS model would need to be modified to evaluate the gradients at each time step, calculate their effect based on the jump distance and direction that is going to be applied, and then modify the jump distance accordingly. We anticipate that a future version of the SDS model will include this capability. For the present users are cautioned to carefully evaluate the results where strong temperature or pressure gradients occur.

The speed with which the SDS method calculates ion trajectories opens up a wide variety of opportunities for investigating systems that hitherto were essentially inaccessible to simulation without extreme expenditure of resources and time. We have chosen to make the model freely available in anticipation that others will find it useful and will share their experiences to help define the scope of its practical application. A listing of the user program with instructions, the statistical definition files, and an example are provided in the Supplementary material. A series of demonstration files are available from the authors.

Acknowledgment

The authors thank M.J. Ward for assistance in mechanical design and fabrication of components of the prototype instrument. This research was supported by the United States Department of Energy under contract DE-AC-07-99ID13727 BBWI.

Appendix A. Supplementary data

Supplementary data associated with this article can be found, in the online version, at doi:10.1016/j.ijms.2005.03.010.

References

[1] A.D. Appelhans, D.A. Dahl, Int. J. Mass Spec. 216 (3) (2002) 269.
[2] J.M. Wells, W.R. Plass, G.E. Patterson, Z. Ouyang, E.R. Badman, R.G. Cooks, Anal. Chem. 71 (1999) 3405.
[3] D.A. Dahl, Int. J. Mass Spectrom. 200 (2000) 3.
[4] ITSIM, http://www.chem.purdue.edu/cooks/ITSIM form.htm.
[5] G.A. Eiceman, Z. Karpas, Ion Mobility Spectrometry, first ed., CRC Press, 1994.
[6] I.R. Gatland, M.G. Thackston, W.M. Pope, F.L. Eisele, H.W. Ellis, E.W. McDaniel, J. Chem. Phys. 68 (1978) 2775.
[7] W.M. Pope, H.W. Ellis, F.L. Eisele, M.G. Thackston, E.W. McDaniel, R.A. Langley, J. Chem. Phys. 68 (1978) 4761.
[8] A.A. Shvartsburg, M.F. Jarrold, Chem. Phys. Lett. 261 (1996) 86.
[9] A.A. Shvartsburg, G.C. Schatz, M.F. Jarrold, J. Chem. Phys 108 (1998) 2416.
[10] G. Balla, A.sD. Koutselos, J. Chem. Phys 119 (2003) 11374.
[11] N. Agbonkonkon, H.D. Tolley, M.C. Asplund, E.D. Lee, M.L. Lee, Anal. Chem 76 (2004) 5223.
[12] SIMION 3D Version 7.0 User's Manual, David A. Dahl, INEL-95/0403 Rev. 5, 2000.
[13] D.A. Dahl, C.L. Atwood, R.A. La Violette, Appl. Math. Model 24 (2000) 771.
[14] W.M. Pope, H.W. Ellis, J.L. Eisele, M.G. Thackston, E.W. McDaniel, J. Chem. Phys. 68 (1978) 4761.
[15] I.R. Gatland, M.G. Thackston, W.M. Pope, J.L. Eisele, H.W. Ellis, E.W. McDaniel, J. Chem. Phys. 68 (1978) 2775.
[16] N. Gee, S.S.-S. Huang, T. Wada, G.R. Freeman, J. Chem. Phys. 77 (1982) 1411.
[17] D.R. Lide (Ed.), Handbook of Chemistry and Physics, 74th ed., CRC Press, 1994.